# Modulation instability in nonlinear coupled resonator optical waveguides and photonic crystal waveguides

**Chih-Hsien Huang,[a] Ying-Hsiuan Lai,[a] Szu-Cheng Cheng,[b] and Wen-Feng Hsieh[a]**

*a) Department of Photonics & Institute of Electro-Optical Engineering,*
*National Chiao Tung University,*
*1001 Tahsueh Rd., Hsinchu 30050, Taiwan*
wfhsieh@cc.nctu.edu.tw
*b) Department of Physics, Chinese Culture University,*
*Yang-Ming Shan, Taipei 111, Taiwan*
sccheng@faculty.pccu.edu.tw

**Abstract:** Modulation instability (MI) in a coupled resonator optical waveguide (CROW) and photonic-crystal waveguide (PCW) with nonlinear Kerr media was studied by using the tight-binding theory. By considering the coupling between the defects, we obtained a discrete nonlinear evolution equation and termed it the extended discrete nonlinear Schrödinger (EDNLS) equation. By solving this equation for CROWs and PCWs, we obtained the MI region and the MI gains, G($p$,$q$), for different wavevectors of the incident plane wave ($p$) and perturbation ($q$) analytically. In CROWs, the MI region, in which solitons can be formed, can only occur for $pa$ being located either before or after $\pi/2$, where $a$ is the separation of the cavities. The location of the MI region is determined by the number of the separation rods between defects and the sign of the Kerr coefficient. However, in the PCWs, $pa$ in the MI region can exceed the $\pi/2$. For those wavevectors close to $\pi/2$, the MI profile, G($q$), can possess two gain maxima at fixed $pa$. It is quite different from the results of the nonlinear CROWs and optical fibers. By numerically solving the EDNLS equation using the 4$^{th}$ order Runge-Kutta method to observe exponential growth of small perturbation in the MI region, we found it is consistent with our analytic solutions.



**OCIS codes:** (190.0190) Nonlinear optics; (130.2790) Guided waves; (230.7370) Waveguides; (230.5298) Photonic crystals.

## References and links

1. E. Yablonovitch, "Photonic band-gap crystals," J. Phys. Condens. Matter **5**, 2443-2460 (1993).
2. E. Yablonovitch, "Photonic band-gap structures," J. Opt. Soc. Am. B **10**, 283-295 (1993).
3. D. W. Prather, S. Y. Shi, J. Murakowski, G. J. Schneider, A. Sharkawy, C. H. Chen, and B. L. Miao, "Photonic crystal structures and applications: Perspective, overview, and development," IEEE J. Sel. Top. Quantum Electron. **12**, 1416-1437 (2006).
4. N. Stefanou and A. Modinos, "Impurity bands in photonic insulators," Phys. Rev. B **57**, 12127-12133 (1998).
5. A. Yariv, Y. Xu, R. K. Lee, and A. Scherer, "Coupled-resonator optical waveguide: a proposal and analysis," Opt. Lett. **24**, 711-713 (1999).
6. A. Imhof, W. L. Vos, R. Sprik, and A. Lagendijk, "Large dispersive effects near the band edges of photonic crystals," Phys. Rev. Lett. **83**, 2942-2945 (1999).
7. W. J. Kim, W. Kuang, and J. D. O'Brien, "Dispersion characteristics of photonic crystal coupled resonator optical waveguides," Opt. Express **11**, 3431-3437 (2003).
8. S. F. Mingaleev, Y. S. Kivshar, and R. A. Sammut, "Long-range interaction and nonlinear localized modes in photonic crystal waveguides," Phys. Rev. E **62**, 5777-5782 (2000).
9. S. F. Mingaleev, and Y. S. Kivshar, "Self-trapping and stable localized modes in nonlinear photonic crystals," Phys. Rev. Lett. **86**, 5474-5477 (2001).

#104106 - $15.00 USD Received 17 Nov 2008; revised 12 Jan 2009; accepted 12 Jan 2009; published 22 Jan 2009

10. D. N. Christodoulides and N. K. Efremidis, "Discrete temporal solitons along a chain of nonlinear coupled microcavities embedded in photonic crystals," Opt. Lett. **27**, 568-570 (2002).
11. S. F. Mingaleev, A. E. Miroshnichenko, Y. S. Kivshar, and K. Busch, "All-optical switching, bistability, and slow-light transmission in photonic crystal waveguide-resonator structures," Phys. Rev. E **74**, 046603 (2006).
12. A. G. Shagalov, "Modulational instability of nonlinear waves in the range of zero dispersion," Physics Lett. A **239**, 41-45 (1998).
13. L. Hadzievski, M. Stepic, and M. M. Skoric, "Modulation instability in two-dimensional nonlinear Schrodinger lattice models with dispersion and long-range interactions," Phys. Rev. B **68**, 014305 (2003).
14. F. K. Abdullaev, A. Bouketir, A. Messikh, and B. A. Umarov, "Modulational instability and discrete breathers in the discrete cubic-quintic nonlinear Schrodinger equation," Physica D-Nonlinear Phenomena **232**, 54-61 (2007).
15. F. M. Mitschke and L. F. Mollenauer, "Discovery of the soliton self-frequency shift," Opt. Lett. **11**, 659-661 (1986).
16. T. Kamalakis and T. Sphicopoulos, "Analytical expressions for the resonant frequencies and modal fields of finite coupled optical cavity chains," IEEE J. Quantum Electron. **41**, 1419-1425 (2005).
17. S. Mookherjea, "Dispersion characteristics of coupled-resonator optical waveguides," Opt. Lett. **30**, 2406-2408 (2005).
18. F. S. S. Chien, J. B. Tu, W. F. Hsieh, and S. C. Cheng, "Tight-binding theory for coupled photonic crystal waveguides," Phys. Rev. B **75**, 125113 (2007).
19. K. Hosomi and T. Katsuyama, "A dispersion compensator using coupled defects in a photonic crystal," IEEE J. Quantum Electron. **38**, 825-829 (2002).

## 1. Introduction

Photonic crystals (PCs) are artificial structures in which the refractive index is periodically distributed at a length scale comparable to the operating wavelength [1, 2]. A photonic crystal waveguide (PCW) can be created by sequentially changing the radii or dielectric constant of the dielectric rods or changing the radii of periodic air holes in a dielectric slab; on the other hand, the coupled resonator optical waveguide (CROW) is created by arranging the cavities, made of point defects, periodically. The electromagnetic (EM) wave can propagate in these channels, PCWs or CROWs, with a very low loss even through a sharp bend [3-5]. However, a pulse experiences serious dispersion in the PCWs and CROWs [6, 7]; therefore, it would hardly propagate within the waveguides without broadening. There are two ideas to improve the situation of allowing the pulse propagation in the waveguides without broadening. The first method is to design a proper structure to create a linear dispersion curve in the range of operating frequency; the second method is to add nonlinear Kerr media to provide solitons propagation [8-11]. However, in the latter case, the criteria of forming a soliton is that the wavevector of the incident wave must be located within the modulation instability (MI) regions [12-14], where the MI refers to a process in which small perturbations upon a uniform intensity beam would grow exponentially [14]. This phenomenon, which is commonly observed in nonlinear optical fibers [15], will also occur in the nonlinear PCWs and CROWs.

Mathematical models of these nonlinear systems often lead to the discrete or continuum-discrete evolution equations such as nonlinear Schrödinger (NLS), sine-Gordon, Klein-Gordon, Korteweg-de Vries and Kadomtsev-Petviashvili equations [13]. In CROWs, the amplitudes of the electric field evolution in the cavities or point defects can be expressed as a discrete NLS equation by using the tight binding theory (TBT) [10, 16, 17] in which the field distribution (or wave function) of an individual cavity is localized at this point defect; thus the coupling between two next nearest-neighbor cavities can be neglected due to long distance. By solving the discrete NLS equation, spatiotemporal discrete solitons can propagate undistorted along a series of coupled resonators or defects by balancing of the effects of discrete lattice dispersion with material nonlinearity [10]. However, it is still lack of the criteria for solitons propagation in different structures of CROWs, e.g., different numbers of separation rods between two cavities with positive or negative Kerr media. Moreover, in the PCWs the defect rods are so close that the next nearest-neighbor coupling cannot be neglected [18] and there are rare reports on pulse propagation in nonlinear PCWs. Therefore, it is needed to take the advanced discussion about different kinds of CROWs and to derive the

#104106 - $15.00 USD Received 17 Nov 2008; revised 12 Jan 2009; accepted 12 Jan 2009; published 22 Jan 2009

extended discrete nonlinear Schrödinger (EDNLS) evolution equation for describing the nonlinear properties in the PCWs.

In this paper, we first use the TBT to describe the EDNLS equation. By considering a small perturbation superimposed on the plane wave solution, the gain of the perturbation which causes the MI can also be derived. Second, by evaluating the coupling coefficients, we shall discuss the regions and gain coefficients of MI in both CROWs and PCWs. In order to verify the correctness of our equations, a CROW and a PCW with square lattices were proposed to calculate the gain coefficients by using the forth-order Runge-Kutta scheme. The simulated results coincide with our analytic analyses.

## 2. Theory

We consider an optical waveguide which consists of a periodic sequence of identical single-mode defects in the PCs with lattice constant $a_L$. The distance between successive defect points or cavities is $a$, and the Kerr media, in which the refraction index is proportional to the intensity of the incident wave, is put in the defect region, shown in Fig. 1. Assuming the isolated point defect is a single mode with eigenfrequency of $\omega_0$, we can express the mode fields of each point defect as $\mathbf{E}(\mathbf{r},t) = \mathbf{E}_0(\mathbf{r})exp(-i\omega_0 t)$ and $\mathbf{H}(\mathbf{r},t) = \mathbf{H}_0(\mathbf{r})exp(-i\omega_0 t)$. The electric field $\mathbf{E}_0'(\mathbf{r},t)$ and magnetic field $\mathbf{H}_0'(\mathbf{r},t)$ of the waveguide can be expressed as a superposition of the bound states, i.e., $\mathbf{E}_0'(\mathbf{r},t) = \sum b_m(t)\mathbf{E}_{0m}$ and $\mathbf{H}_0'(\mathbf{r},t) = \sum b_m(t)\mathbf{H}_{0m}$, where $\mathbf{E}_{0m} = \mathbf{E}_0(\mathbf{r}-ma)$ and $\mathbf{H}_{0m} = \mathbf{H}_0(\mathbf{r}-ma)$.

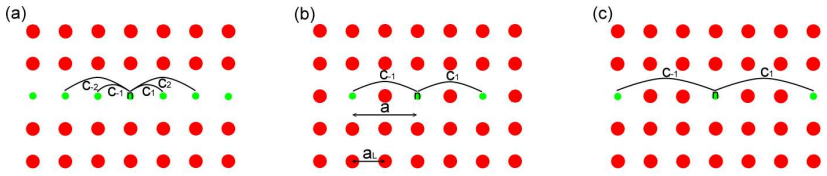


Fig. 1. The structures of (a) a PCW, (b) a CROW with one separation rod and (c) a CROW with two separation rods, where a is the length of successive defect points and $a_L$ is the lattice constant of a PC.

Under the tight-binding approximation, we consider the couplings up to the next nearest-neighbor defects and obtain the EDNLS equation as [18]

$$i\frac{db_n}{dt} + (-\omega_0 + c_0)b_n + c_1(b_{n+1} + b_{n-1}) + c_2(b_{n+2} + b_{n-2}) + \gamma|b_n|^2 b_n = 0. \quad (1)$$

Here the linear coupling coefficient $c_m$ is defined as [10]

$$c_m = \frac{\omega_0 \iiint d\upsilon \Delta\varepsilon E_{0n} \cdot E_{0n+m}}{\iiint d\upsilon(\mu_0|H_{0n}|^2 + \varepsilon|E_{0n}|^2)}, \quad (2)$$

with $\Delta\varepsilon(\mathbf{r}) = \varepsilon'(\mathbf{r}) - \varepsilon(\mathbf{r})$ being the difference of dielectric constants of the waveguide ( $\varepsilon'(\mathbf{r})$ ) and the point-defected PC ( $\varepsilon(\mathbf{r})$ ) and $c_0$ representing a small shift in the eigenfrequency $\omega_0$ that arises from present of the neighbor defects or cavities. The self-phase modulation strength $\gamma$ is given by

$$\gamma = \frac{2n_0 n_2 \varepsilon_0 \omega_0 \iiint d\upsilon|E_{0n}|^4}{\iiint d\upsilon(\mu_0|H_{0n}|^2 + \varepsilon|E_{0n}|^2)}, \quad (3)$$

with $n_2$ being the Kerr coefficient. Let the plane wave with amplitude $\phi_0$, propagation wavevector $p$, and frequency $\omega$ in site n as $b_n = \phi_0 exp(inpa - i\omega t)$ be the solution of Eq. (1). The dispersion relation of the nonlinear PCW can be derived as

#104106 - $15.00 USD Received 17 Nov 2008; revised 12 Jan 2009; accepted 12 Jan 2009; published 22 Jan 2009

$$\omega(pa) = \omega_0 - c_0 - 2c_1\cos(pa) - 2c_2\cos(2pa) - \gamma\,|\phi_0|^2 . \quad (4)$$

Considering a small perturbation $v_n(t)$ superimposed on a plane wave, shown as [14]

$$b_n = (\phi_0 + v_n(t))e^{i(pna-\omega t)}, \quad (5)$$

we can substitute Eq. (5) into Eq. (1) to get

$$\begin{aligned} & i\frac{dv_n}{dt} + c_1(v_{n+1}e^{ipa} + v_{n-1}e^{-ipa} - 2\cos(pa)v_n) + \\ & c_2(v_{n+2}e^{ipa} + v_{n-2}e^{-ipa} - 2\cos(2pa)v_n) + \gamma|\phi_0|^2(v_n + v_n^*) = 0. \end{aligned} \quad (6)$$

Taking $v_n(t)$ as this form [14]

$$v_n(t) = (V_1 e^{iqna} + V_2^* e^{-iqna})e^{-i\Omega t}, \quad (7)$$

where $q$ and $\Omega$ are the wavevector and frequency of the modulation perturbation. $V_1$ and $V_2^*$ represent small perturbation with perturbation wavevectors of $q$ and $-q$. Substituting $v_n(t)$ into Eq.(6), we osbtioned the dispersion relation of the perturbation:

$$\Omega(p,q) = B \pm \sqrt{A(A - \gamma\,|\phi_0|^2)}\,, \quad (8)$$

where $A = 4c_1\cos(pa)\sin^2(\frac{qa}{2}) + 4c_2\cos(2pa)\sin^2(qa)$ and $B = 2c_1\sin(pa)\cos(qa) + 2c_2\sin(2pa)\cos(2qa)$. If the dispersion relation $\Omega(p,q)$ is complex as $A(A - \gamma|\phi_0|^2) < 0$, the perturbation field would become unstable. The intensity growing rate G of MI, also called the MI gain, is related to the imaginary part of $\Omega(p, q)$, i.e.,

$$G(p,q)=2*\mathrm{Im}(\Omega(p,q)) = \mathrm{Re}(2\cdot\left|A(\gamma|\phi_0|^2 - A)\right|^{\frac{1}{2}}) = 2\cdot\mathrm{Re}\sqrt{-(A - 0.5\gamma|\phi_0|^2)^2 + 0.25\gamma^2|\phi_0|^4}\,. \quad (9)$$

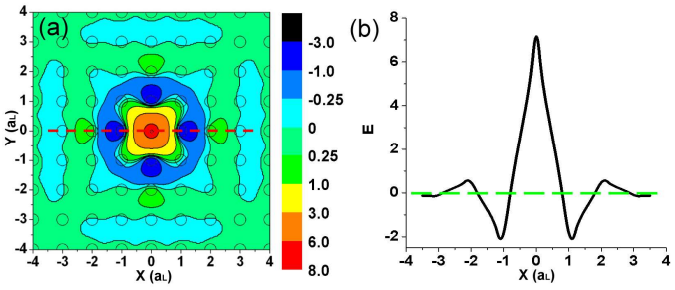


Fig. 2. (a) The electric field distribution ($E_z$) of point defect mode simulated by the plane wave expansion method in the square lattice with the dielectric constant, radii of dielectric rods and the radius ($r_d$) of the defect rods being 12 , $0.2a_L$ and $0.05a_L$ for frequency f = 0.364 $c/a_L$ . (b) The field distribution of the red dash line in (a).

### 3. Analyses and discussion

In this section, we will further discuss about the MI regions and gains in both CROWs and PCWs made of point defects, shown in Fig. 1. The electric field distribution ($E_z$) of a single point defect, simulated by the plane wave expansion method in the square lattice with the dielectric constant, radii of dielectric rods and the radius ($r_d$) of the defect rods being 12, $0.2a_L$ and $0.05a_L$ for frequency f = 0.364 $c/a_L$ is shown in Fig. 2. And the field profile along the red dash line in Fig. 2(a) is plotted in Fig. 2(b), it has the opposite sign when it extends to the nearest-neighbor defects for the PCW ($\mathbf{E}_0(0,0)*\mathbf{E}_0(a_L,0) < 0$) and the CROW ($\mathbf{E}_0(0,0)*\mathbf{E}_0(3a_L,0) < 0$) with even (2) separation rods. To maintain a single mode propagating in the waveguides, the radii or the refraction index of the rods in the waveguides is reduced therefore $\Delta\varepsilon$ is negative in the following discussion. Since the electric field is mainly localized around the dielectric rods of the waveguides, we can use the maximum values to

#104106 - $15.00 USD Received 17 Nov 2008; revised 12 Jan 2009; accepted 12 Jan 2009; published 22 Jan 2009

replace the integral values for a simple estimation in Eq. (2). Therefore, $c_1$ is positive in even-separated-rod CROWs [16]. However, $c_2$ would be two orders of magnitude smaller than $c_1$ so that we considered only the nearest-neighbor coupling in the CROWs and let $c_2 \approx 0$ [10, 18]. On the other hand, $\mathbf{E}(0,0)^*\mathbf{E}(2a_L,0)$ is positive in the odd-separation-rod (1) CROWs so $c_1$ would be negative and $c_2 \approx 0$.

Because of $c_2 \approx 0$ for the CROWs, the coefficient $A$ can be rewritten as $A = 4c_1 \cos(pa)\sin^2(qa/2)$, in which the sign of $A$ is determined only by $pa$ and it changes sign at $pa = \pi/2$. Here the region of $pa$ (or $qa$) is defined between 0 and $\pi$. For positive (negative) $A$, $\gamma$ must also be positive (negative) and $\gamma|\phi_0|^2 > A > 0$ ($\gamma|\phi_0|^2 < A < 0$) to support MI, which can be easily derived by Eq. (9); in other words, $c_1\cos(pa)\gamma$ must be positive in MI region. Therefore, the boundary of MI must be located at $pa = \pi/2$. In odd-separation-rod CROWs, $c_1$ is negative, therefore $A$ and $\gamma$ must be both negative when $0 < pa < \pi/2$ and positive as $pa > \pi/2$. However, in even-separation-rod CROWs, $c_1$ is positive, therefore $A$ and $\gamma$ must be both positive when $0 < pa < \pi/2$ and negative as $pa > \pi/2$, shown in Table 1. When the structure of the waveguide ($c_1$) has been chosen, $|A|$ increases if $q$ increases at constant $c_1$ and $p$. When we plot the gain profile as the graph of G vs. $q$ at a given $p$ and defined the gain maximum as the maximal values in the graph, from Eq. (9), the gain maximum would be located at $A = 0.5\gamma|\phi_0|^2$ and cut off at $A = \gamma|\phi_0|^2$ when $4|c_1\cos(pa)| > 0.5|\gamma|\left|\phi_0\right|^2$; otherwise, the gain maximum would be located at $qa = \pi$.

Table 1 MI regions of CROWs

| Separation rods | Sign of $c_1$ | Sign of $n_2(\gamma)$ | MI regions ($pa$) |
|---|---|---|---|
| Odd | - | + | $> \pi/2$ |
| | | - | $< \pi/2$ |
| Even | + | + | $< \pi/2$ |
| | | - | $> \pi/2$ |

In negative (positive) $c_1$ for an odd-separation-rod (even-separation-rod) case, the dispersion relation slop is negative (positive) [19] and the frequency dispersion D defined as $d^2\omega/dk^2$ is negative (positive) when $pa < \pi/2$ and positive (negative) for $pa > \pi/2$ from Eq. (4). Therefore, for negative D ($pa < \pi/2$ for the odd-separation-rod case and $pa > \pi/2$ for the even-separation-rod case), the negative $\gamma$ is needed to support MI and positive $\gamma$ is needed to support MI for positive D. In other words, the MI regions of the CROWs in $pa$ can also be decided by simply considering the parameters of D and $\gamma$.

On the other hand, $\mathbf{E}_n\mathbf{E}_{n+1}$ or $\mathbf{E}_0(0,0)^*\mathbf{E}_0(a_L,0) < 0$ and $\mathbf{E}_n\mathbf{E}_{n+2} > 0$ in PCWs with $a_L = a$, therefore, $c_1$ is positive and $c_2$, which cannot be neglected, is negative. First, we consider the positive Kerr media having positive $n_2$ (or $\gamma$) so the criterion of the MI is $\gamma|\phi_0|^2 > A > 0$. From the criterion of $A = 4c_1\cos(pa)\sin^2(qa/2) + 4c_2\cos(2pa)\sin^2(qa) > 0$, since $c_2$ is an order of magnitude smaller than $c_1$, this criterion can be further reduced to $\cos(pa) > -4|c_2/c_1|\cos^2(qa/2)$. Under this circumstance, the MI region is determined not only by $pa$ but also by $qa$, and $pa$ in the MI region can exceed $\pi/2$, unlike in CROWs that the MI boundary for $pa$ is located at $\pi/2$ and is independent of $qa$. From the other criterion: $\gamma|\phi_0|^2 > A$, we found A is dominated by the $c_1$ term as $pa$ is located away from $\pi/2$, in this case the MI gain is similar to that in the CROWs with even separation rods. Contrarily, when $pa$ approaches to $\pi/2$, the $c_1$ term is almost zero and $A$ becomes dominated by the $c_2$ term. In this case, $A$ would not increase as increasing $qa$. From Eq. (9), we knew that the maximum of the gain profile, G(q), is located at $A = 0.5\gamma|\phi_0|^2$ or $dA/dq = 0$. For the latter case, the peak gain would be

#104106 - $15.00 USD Received 17 Nov 2008; revised 12 Jan 2009; accepted 12 Jan 2009; published 22 Jan 2009

smaller than that of the former condition. When $4c_2 \cos(2pa) < 0.5\gamma|\phi_0|^2$, there would be two gain maxima at a fixed $pa$ and the gain maxima is located at $A = 0.5\gamma|\phi_0|^2$, but there would be only one gain maximum located at $dA/dq = 0$ as $4c_2 \cos(2pa) < 0.5\gamma|\phi_0|^2$.

On the other hand, in the condition of negative γ, the first criterion is $\cos(pa) < -4|c_2/c_1| \cdot \cos^2(qa/2)$. We found the MI would happen only when $pa > \pi/a$. However, when $0 > \cos(pa) > -4|c_2/c_1|$, the MI region is located at the higher $q$ rather than the general case in which the perturbation would have gain at $qa = 0^+$. The cutoff gain is also decided by $A = \gamma|\phi_0|^2$.

## 4. Simulation results

We consider a square lattice PC with the dielectric constant and radii of the dielectric rods being 12 and $0.2a_L$, where $a_L$ is the lattice constant of the PCs. The radii ($r_d$) of the defect rods are reduced to be $0.05a_L$ and the Kerr media are introduced around the defects between one separation rod to create the CROW and sequentially to create the PCW. The structures and dispersion relations of the CROW and PCW in TM polarization (the electric field parallels the rod axis) without Kerr media are shown in Fig. 3, which are simulated by the plane wave expansion method.

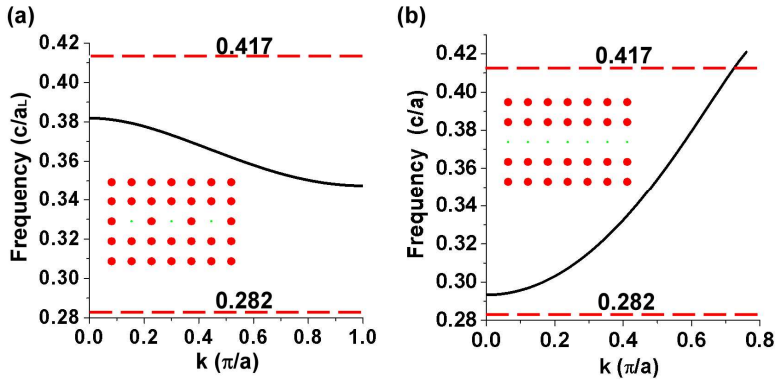


Fig. 3. The dispersion relations of (a) a CROW with one separation rod and (b) a PCW in square lattices, which are simulated by the plane wave expansion method. The dash red lines are the edges of the band gaps.

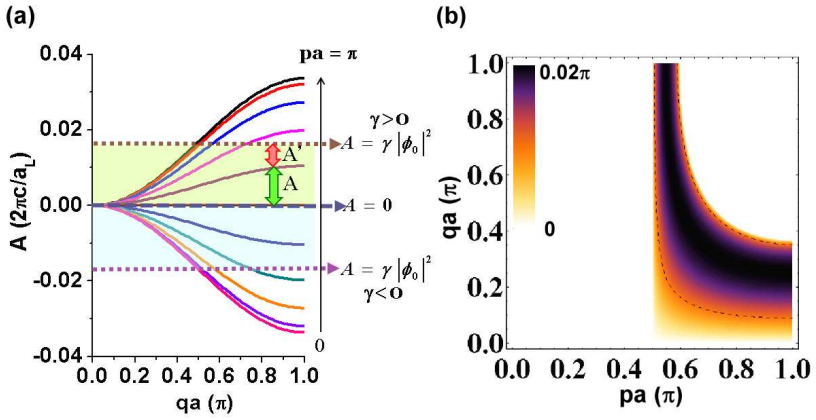


Fig. 4. (a) The values of A and (b) the gains and regions of the MI of the CROW with $\gamma|\phi_0|^2=0.01$ ($2\pi c/a_L$).

#104106 - $15.00 USD Received 17 Nov 2008; revised 12 Jan 2009; accepted 12 Jan 2009; published 22 Jan 2009

First, the properties of the MI in the CROW would be discussed. The coupling coefficient $c_1$ is -0.00841 ($2\pi c/a_L$), where c is the speed of light in the vacuum. Because $c_1$ is negative, the eigenfrequencies will decrease as increasing k. Figure 4(a) shows $A$ vs. $qa$ with different $p$. Let $A'$ be $\gamma|\phi_0|^2$ - $A$ so that $G = 2\sqrt{AA'}$. As aforementioned, the MI region is determined by the condition that $A$ lies between 0 and $\gamma|\phi_0|^2$ and the maximum of G appears when $A$ equals (or is the closest) to $0.5\gamma|\phi_0|^2$. Figure 4(b) shows $G(p,a)$ with $\gamma|\phi_0|^2$=0.01 ($2\pi c/a_L$). It can be seen that there is no MI gain when $pa \le 0.5\pi$ and only a single gain maximum at given $pa$ in the condition of $pa > 0.576\pi$.

In PCWs, the coupling coefficients of $c_1$ and $c_2$ are 0.039 and -0.0047($2\pi c/a$), and $\omega_0$-$\Delta\omega$ is 0.3632 ($2\pi c/a$). The values of $A$ at a given $pa$ were shown in Fig. 5(a). When $pa$ is small, i.e., in [0, 0.4$\pi$], $A$ is dominated by $c_1$ term and $A$ increases as $qa$ increases. Due to $c_1$ is positive, the properties of MI would be similar to the CROWs with even separation rods that possesses a single gain maximum as the solid curve in Fig. 6(a) for $pa = 0.4\pi$. However, as $pa$ is in (0.4$\pi$, 0.6$\pi$], $A$ is not simple increasing or decreasing function of $qa$, shown in Fig. 5(b). At a given $pa$ with positive Kerr media ($\gamma > 0$), when the values of A(q) is always smaller than $0.5\gamma|\phi_0|^2$, e.g., $\gamma|\phi_0|^2 = 0.01$ ($2\pi c/a$) and $pa = 0.6\pi$, there would be a maximal gain as the solid curve in Fig. 6(d). However, when A(q) is larger than $0.5\gamma|\phi_0|^2$, e.g., $\gamma|\phi_0|^2$=0.01 ($2\pi c/a$) and $pa = 0.49\pi$ and $0.55\pi$, there would have 2 gain maxima, solid curves shown in Fig. 6(b) and (c). And the MI region with positive $\gamma$ can extend to $pa = 0.6\pi$, as shown in Fig. 5(c). On the other hand, the MI region with negative Kerr media is shown in Fig. 5(d) which is located within $\pi/2 < pa < \pi$ but having the MI region located at high $qa$ as $pa$ close to $\pi/2$.

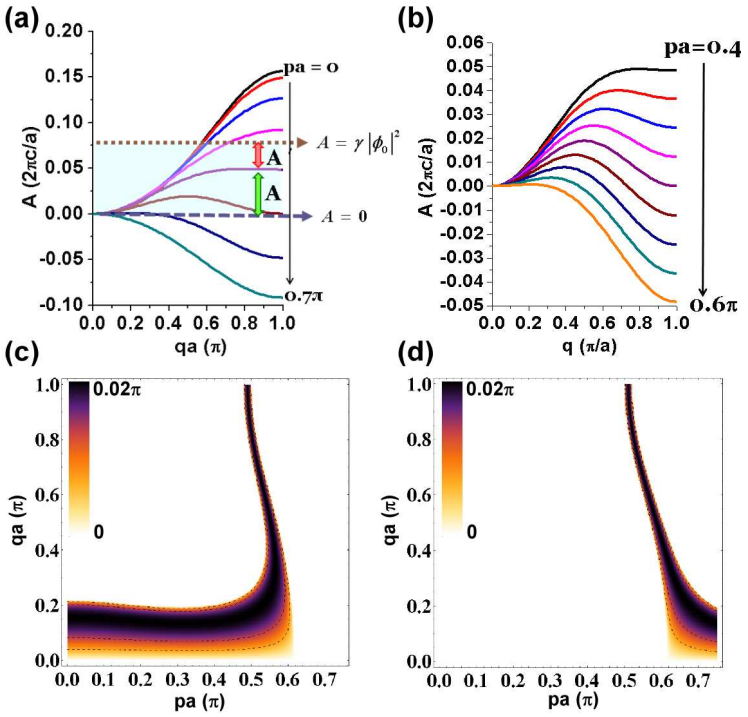


Fig. 5. (a) (b)The values of A in the PCW. The region and gains of MI with (c) positive Kerr media ($\gamma|\phi_0|^2$=0.01*2πc/a) and (d) negative Kerr media ($\gamma|\phi_0|^2$=-0.01*2πc/a).

Next, we would use the 4th order Runge-Kutta method to simulate the evolution of the perturbation. A plane wave with 10% initial sinusoidal perturbation is used as the input

#104106 - $15.00 USD Received 17 Nov 2008; revised 12 Jan 2009; accepted 12 Jan 2009; published 22 Jan 2009

source in a square-array PCW with $\gamma|\phi_0|^2 = 0.01$ ($2\pi c/a$). The perturbation will grow exponentially in the MI region to become a discrete soliton before it splits, as shown in Fig. 7(a), but the perturbation would never grow outside the MI region in Fig. 7(b). We plot the gain coefficients with square dots in Fig. 6 by evaluating the growing rate by the Runge-Kutta method and then compare with gain profiles (solid curves) calculated by using Eq. (9). The results show a quite good agreement.

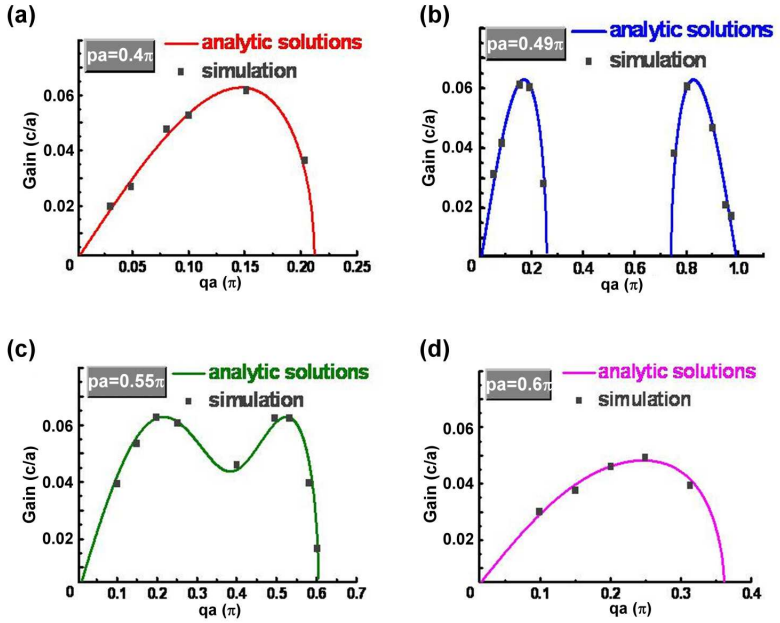


Fig. 6. The MI gain profiles gotten by analytic solution and the simulation by 4th order Runge-Kutta method in different qa with $\gamma|\phi_0|^2 = 0.01$ ($2\pi c/a$).

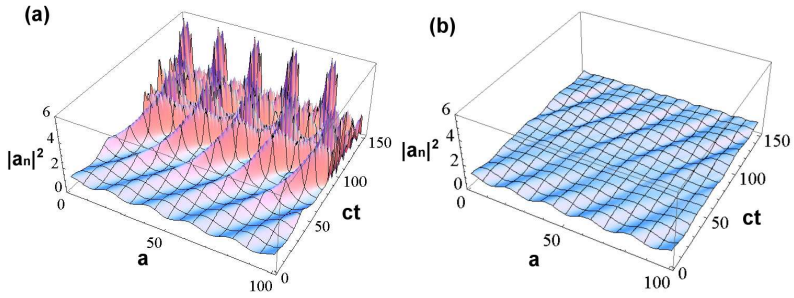


Fig. 7. The evolution of the perturbation in the PCW with (a) pa=0.4π and qa=0.1π (b) pa=0.6π and qa=0.1π.

## 5. Conclusion

We have successfully used the TBT to investigate MI in both CROWs and PCWs by considering growth of a small perturbation superimposed on a plane wave. The number of separation rods in the CROWs would decide the signs of the nearest-neighbor coupling coefficients ($c_1$) and the next nearest-neighbor coefficient ($c_2$) can be neglected because it is more than 2 orders of magnitude smaller than $c_1$. This leads to positive dispersion for positive

#104106 - $15.00 USD Received 17 Nov 2008; revised 12 Jan 2009; accepted 12 Jan 2009; published 22 Jan 2009

coupling coefficient and vice versa. Although the signs of the coupling coefficient could be different, the criteria: $c_1\cos(pa)\gamma > 0$ for obtaining modulation instability is the same for incident plane wave of wavevector $p$. Therefore, the MI region can only be located in either $pa < \pi/2$ or $pa > \pi/2$ with only one gain maximum. In the air-defect PCWs, $c_1$ is positive and $c_2$, which is no longer negligible, is negative. It makes the MI gain of positive Kerr media located at low wavevectors in the first Brilluoin zone and vice versus. The boundary of gain region of $pa$ is not exactly at $\pi/2$ due to the MI is mainly dominated by $c_2$ term as $pa$ approaches $\pi/2$ and there could exist two gain maxima. Furthermore, the numerical simulation using the $4^{th}$ order Runge-Kutta method reveals exponentially growing perturbation intensity as it propagates and the growing rate matches with the gain coefficient of MI in the analytic solution.

**Acknowledgments**

The authors would like to thank the National Science Council of the Republic of China for partial financial support under grants NSC96-2628-M-009-001-MY3, NSC96-2112-M-034-002-MY3, and NSC96-2628-E-009-018-MY3. Mr. Chih-Hsien Huang would like to thank NSC for providing fellowship.

#104106 - $15.00 USD Received 17 Nov 2008; revised 12 Jan 2009; accepted 12 Jan 2009; published 22 Jan 2009